

New techniques for chargino-neutralino detection at LHC

Maria Eugenia Cabrera

*University of Amsterdam
Institute of Theoretical Physics
GRAPPA
E-mail: M.E.CabreraCatalan@uva.nl*

J. Alberto Casas

*Instituto de Física Teórica, IFT-UAM/CSIC
U.A.M., Cantoblanco,
28049 Madrid, Spain
E-mail: alberto.casas@uam.es*

Bryan Zaldivar

*Instituto de Física Teórica, IFT-UAM/CSIC
U.A.M., Cantoblanco,
28049 Madrid, Spain
E-mail: b.zaldivar.m@csic.es*

ABSTRACT: The recent LHC discovery of a Higgs-like boson at 126 GeV has important consequences for SUSY, pushing the spectrum of strong-interacting supersymmetric particles to high energies, very difficult to probe at the LHC. This gives extra motivation to study the direct production of electroweak particles, as charginos and neutralinos, which are presently very poorly constrained. The aim of this work is to improve the analysis of chargino-neutralino pair production at LHC, focusing on the kinematics of the processes. We propose a new method based on the study of the *poles* of a certain kinematical variable. This complements other approaches, giving new information about the spectrum and improving the signal-to-background ratio. We illustrate the method in particular SUSY models, and show that working with the LHC at 100/fb luminosity one would be able to distinguish the SUSY signal from the Standard Model background.

KEYWORDS: Beyond Standard Model, Collider physics, Supersymmetry Searches, Kinematic Variables, LHC physics, chargino neutralino production.

Contents

1. Introduction	1
2. State of the art of the analysis	3
3. Our Strategy	4
3.1 The visible transverse energy	4
3.2 From CM_χ to LAB	5
4. Testing the efficiency of E_T^v and p_T^v in concrete SUSY models	10
5. Conclusions	16

1. Introduction

The recent discovery of the Higgs boson, with a mass around 126 GeV [1], [2], does not only have crucial importance by itself. It also has far-reaching consequences for well-motivated candidates for physics beyond the Standard Model (SM), such as Supersymmetry (SUSY), and in particular the Minimal Supersymmetric Standard Model (MSSM). As it is well known, such a value requires large radiative corrections, which go with (the logarithm of) the supersymmetric masses, in particular with the stop masses. Consequently, the latter must be rather high (well above 1 TeV unless the stop mixing is close to the maximal value), thus suggesting that the mass scale of SUSY particles could be substantially higher than expected from fine-tuning arguments. This would also make very challenging, if not impossible, to detect SUSY at LHC in a direct or indirect way. In fact, this is already the most likely situation for the constrained MSSM [3, 4, 5, 6, 7, 8, 9], i.e. assuming universality of soft terms at a high-scale.

Prospects become much more interesting if some supersymmetric states remain sufficiently light, which in general implies to go beyond the constrained MSSM. An attractive possibility in this sense is that charginos and neutralinos are substantially lighter than sfermions. This scenario is supported not only by the phenomenological fact that the present bounds on charginos and neutralinos are pretty mild. There are also some theoretical and phenomenological motivations to explore this possibility. Namely, the successful supersymmetric unification of the gauge couplings requires light supersymmetric fermions. Besides, heavy sfermions are welcome to suppress dangerous flavor-violation effects. Another motivation comes from dark matter (DM) constraints. The last data of XENON100 in combination with the Higgs mass have narrowed enormously the MSSM candidates for DM, see e.g. refs.[3, 9]. Probably the most satisfactory scenario that survives occurs when

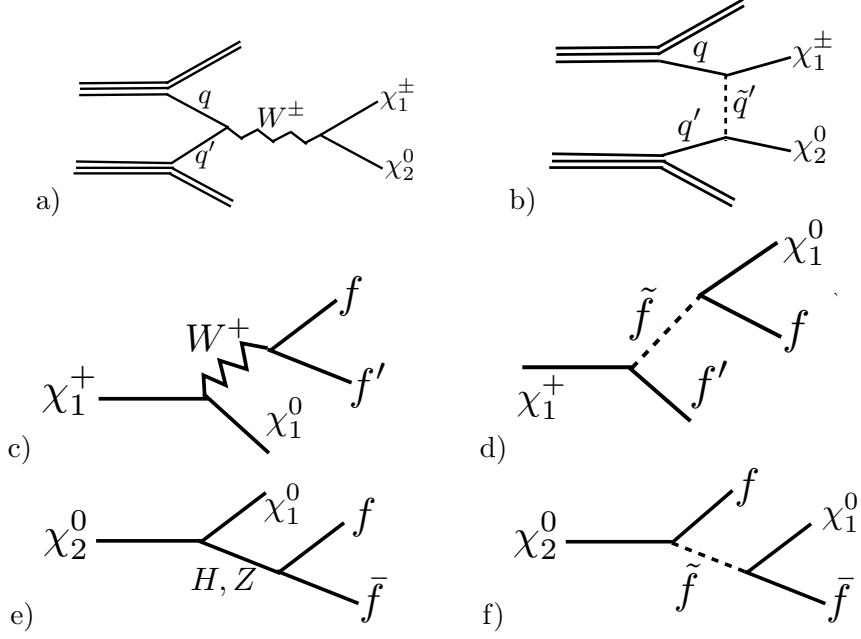


Figure 1: a) and b) Typical production processes of a pair $\chi_1^\pm \chi_2^0$ in the LHC. c) and d) Chargino decay modes. e) and f) Neutralino decay modes.

the lightest neutralino is almost pure Higgsino with a mass around 1 TeV. But if gaugino masses are not universal there are other possibilities. Namely, one can have a much lighter (mostly bino) neutralino which annihilates in the early universe through a combination of Z -boson and Higgs funnels, see [3]. It can also co-annihilate with e.g. sleptons if their masses are close enough. Another alternative is that the LSP neutralino is mostly wino, in which case the co-annihilation with the lightest chargino becomes important.

In summary, a scenario where all the supersymmetric particles are too heavy, except charginos and neutralinos (and maybe gluinos), is plausible and has interesting motivations. Therefore it would be worthy to improve the present techniques to analyze the production and detection of chargino/neutralino pairs at the LHC; and this is the main motivation of this paper.

In most of the cases the chargino-neutralino pair created is $\chi_1^\pm \chi_2^0$, i.e. the lightest chargino and the next-to-lightest neutralino. Some of the diagrams of production and decay are shown in Fig. 1. The chargino and the neutralino can decay in several ways, always giving an LSP (χ_1^0) at the end of each cascade.

The study of chargino-neutralino pair production has been performed previously in e.g. [10], [11], [12] through the analysis of leptonic final states. The aim of our work is to improve those analyses, by proposing new strategies which are complementary and more efficient in some cases¹. Our analysis is by construction independent of the diagrams through which the chargino and the neutralino decay, since it is entirely based on the properties of the final states. It can also be applied to final states including hadrons, such as $b\bar{b}\ell$.

¹For a general review on kinematical techniques, see [13].

The outline of the paper is as follows. In section 2 we describe the present status of the analyses of possible chargino-neutralino production and detection, as done by ATLAS and CMS groups, and motivate the convenience of improving this kind of analysis. In section 3 we describe our strategy, by proposing a kinematical variable which allows to obtain direct information about the SUSY spectrum. It is also very useful to concentrate signal-events, thus improving the S/B ratio, and thus the LHC potential for discovery of new physics. Section 4 is devoted to illustrate the use of this variable in concrete SUSY models. We finally conclude in section 5.

2. State of the art of the analysis

As shown in Fig.1, the neutralino χ_2^0 can decay through a charged sfermion, a Higgs or a Z -boson, depending on the kinematical availability and the χ_2^0 composition. Likewise, the chargino χ_1^\pm can decay, among other channels, through a charged sfermion or a W -boson. However, as long as the sleptons are heavier than χ_2^0 and χ_1^\pm , these decay channels become very suppressed and the decays through on-shell Higgs, Z and W dominate.

Ref. [10] contains a study of purely leptonic final states of the type $\ell^+\ell^-\ell'^\pm$, where ℓ and ℓ' may be identical leptons. The authors perform separate analyses of two cases: 1) the invariant mass of identical opposite-sign leptons ($m_{\ell^+\ell^-}$) does *not* reproduce the Z -boson mass, M_Z , and 2) it does. They assume that the χ_2^0 decays through a slepton (case 1) or a Z -boson (case 2). In both cases, they use the E_T^{miss} variable to compare the actual experimental data with the SM background, finding no significant excess of events so far, once all the uncertainties are taken into account. The negative result is then interpreted as contour bounds in the parameter space of e.g. concrete simplified models.

A very complete analysis was presented later in ref.[11]. Again, the authors focus on 3-lepton final states, but using either the variable E_T^{miss} or $m_{\ell^+\ell^-}$ in combination with M_T (the transverse mass built with the momentum of the unpaired lepton) and E_T^{miss} . One option gives better sensitivity than the other, depending on the mass splittings between χ_1^0 and its respective mothers. A second analysis was performed for 2-lepton final states, considering the possibility that one of the 3 leptons produced by χ_1^\pm or χ_2^0 may be lost or does not pass the kinematical cuts. In a last analysis they considered that both χ_1^\pm and χ_2^0 may decay through on-shell vector bosons, giving $2\ell + 2j$ in the final state, for which the SM background has not intrinsic E_T^{miss} . Using these techniques they were able to provide contour bounds on χ_1^\pm , χ_2^0 and χ_1^0 masses for particular simplified models.

A quite efficient analysis of the decay through sleptons was presented in ref. [12] (based on [14] and [15]), where the authors used the $m_{\ell^+\ell^-}$ variable. An obvious advantage of this choice is that $m_{\ell^+\ell^-}$ is Lorentz invariant and thus the analysis is fully valid in the (boosted) LAB frame. It can be shown that, when the intermediate sleptons are produced on-shell, the histogram on $m_{\ell^+\ell^-}$ has an edge at a value given by a certain combination of the χ_2^0 , χ_1^0 and $\tilde{\ell}$ masses[14],[16],[17]. This potentially gives a very distinctive experimental signal. When the sleptons are produced off-shell, the authors use a strategy based on the

study of end-points in $m_{\ell^+\ell^-}$. This case is much less efficient, since by definition one has poorer statistics and a more difficult-to-control background.

In this paper we propose the use of a variable whose distinctive feature is to concentrate the signal events around a peak, not relying on end-points. It also provides direct information about the spectrum. Besides, it can be applied without any assumption or guess about the decay mode that takes place (through Z -boson, sleptons, Higgs or whatever). We describe the idea in the next section.

3. Our Strategy

3.1 The visible transverse energy

In contrast with the previous analyses, our strategy is purely kinematical and based only on the characteristics of the initial (χ_2^0) and the final states ($f\bar{f}\chi_1^0$); so it is independent of the channel through which the χ_2^0 decays. As it is based just on the χ_2^0 -chain, the analysis can be easily combined with other analyses that use partial information from both the χ_2^0 and the χ_1^\pm chains. It can also be applied to other processes where one or two χ_2^0 states are produced.

We initially work in the reference frame in which χ_2^0 is at rest, which we call $\text{CM}\chi$ (do not confuse with the center-of mass of the partonic collision) and consider the \mathcal{E}_T variable, defined as

$$\mathcal{E}_T = \hat{E}_T^v + \hat{E}_T^\chi \quad (3.1)$$

where \hat{E}_T^v , \hat{E}_T^χ are the transverse energies of the visible system (e.g. $v \equiv \ell^+\ell^-$) and the missing system,

$$\hat{E}_T^v = \sqrt{M_v^2 + (\hat{p}_T^v)^2}, \quad \hat{E}_T^\chi = \sqrt{M_\chi^2 + (\hat{p}_T^\chi)^2} \quad (3.2)$$

Here M_v and M_χ are the invariant masses of the visible system and the LSP (χ_1^0) and hats denote $\text{CM}\chi$ quantities everywhere. Of course, $(\hat{p}_T^v)^2 = (\hat{p}_T^\chi)^2$.

As it has been discussed in ref. [18], the histogram of events displayed in the \mathcal{E}_T variable has a pole at the mass of χ_2^0 ,

$$\mathcal{E}_T|_{\text{pole}} = E_{\text{CM}\chi} = M_{\chi_2} \quad (3.3)$$

Besides, for $\mathcal{E}_T > M_2$ there are no events, so the histogram has an sharp edge at the pole. Hence, potentially, the \mathcal{E}_T variable can give a very distinctive signal, well separated from the background, providing in addition direct information about the SUSY spectrum. Note also that \mathcal{E}_T is invariant under longitudinal boosts. There are however some problems. First, even working at the $\text{CM}\chi$ frame, i.e. assuming that χ_2^0 was produced with vanishing transverse momentum, we cannot measure the invisible transverse energy, E_T^χ , due to the uncertainty on the value of M_χ . Actually, we have checked that in general $M_\chi \simeq 0$ is not a good approximation. Second, the χ_2^0 neutralino is usually produced with a non-vanishing transverse momentum. We postpone the second issue to the next subsection and focus now on the first one.

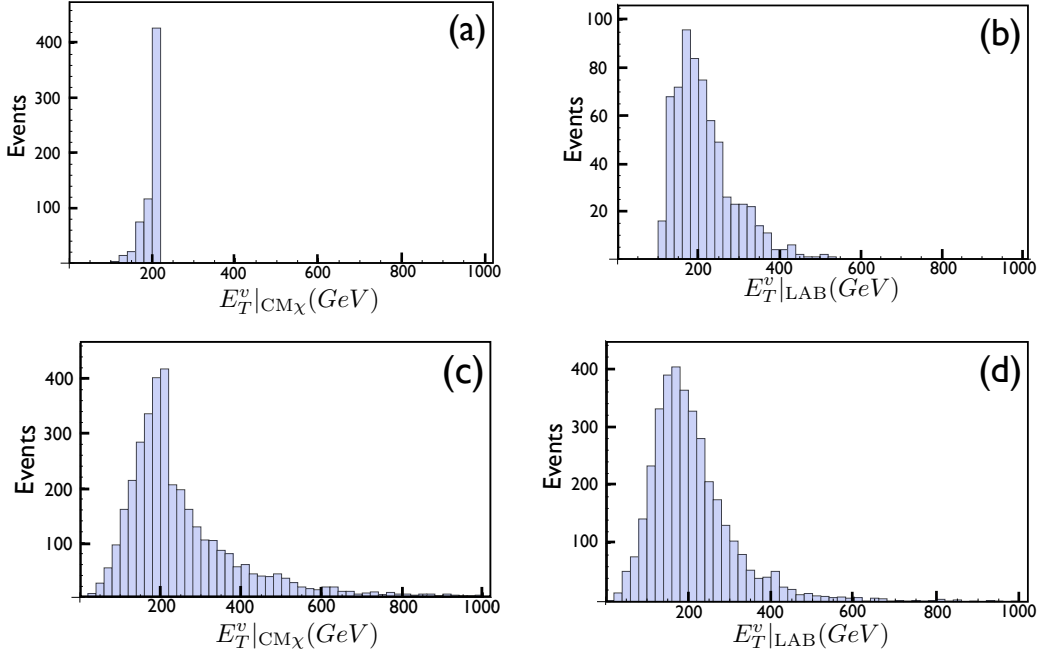


Figure 2: Histogram (number of events) of E_T^v in the cases where v is a) a $\tau\bar{\tau}$ pair in the $\text{CM}\chi$ frame; b) a $\tau\bar{\tau}$ pair in the LAB frame; c) a $j_b j_b$ pair in the $\text{CM}\chi$ frame, and d) a $j_b j_b$ pair in the LAB frame. The details of the SUSY point correspondent to this histograms are described in the text.

In order to avoid the dependence on unknown quantities, a good strategy is to work just with the visible transverse energy, E_T^v , defined in eq.(3.2). It can be easily checked that the pole in the \mathcal{E}_T variable, eq.(3.3), translates into a pole in \hat{E}_T^v ,

$$\hat{E}_T^v \Big|_{\text{pole}} = \frac{1}{2M_{\chi_2}} [M_{\chi_2}^2 - M_\chi^2 + M_v^2] \quad (3.4)$$

In general, the mass of the visible system, M_v , can change from event to event. However, if χ_2^0 decays through a Higgs (very common case) or through a Z -boson, all the events are concentrated around $M_v = m_h$ (M_Z). An example of this kind, which shows clearly the edge and pole in the $\text{CM}\chi$ frame can be seen in the plot a) of Fig.2, to be discussed below in more detail. When χ_2^0 decays through sleptons, we can select a fraction of the events with similar M_v , and check that in $\text{CM}\chi$ a pole appears as in (3.4). This decreases the statistics but not in a dramatic way. Actually, in cases where $M_v^2 \ll M_{\chi_2}^2$, one could do a histogram with all the events, since the pole appears then around $\hat{E}_T^v \simeq \frac{1}{2M_{\chi_2}} (M_{\chi_2}^2 - M_\chi^2)$. Next, we study what happens when we go from the $\text{CM}\chi$ to the actual LAB frame.

3.2 From $\text{CM}\chi$ to LAB

The clean and sharp behavior of the \hat{E}_T^v variable in $\text{CM}\chi$ becomes of course less keen-edged when passing to the LAB frame. This is illustrated by the plots of Fig. 2. They correspond to a CMSSM model with $m_0 = 500$ GeV, $M_{1/2} = 700$ GeV, $\tan \beta = 10$, $A_0 = 0$, and $\mu > 0$. The associated relevant spectrum for us is $M_{\chi_2} \approx 554$ GeV and $M_\chi \approx 294$

GeV. The χ_2^0 neutralino decays almost entirely through an on-shell Higgs. In the CM χ frame the pole for E_T^v , eq. (3.4), is at ~ 210 GeV. We have simulated the events using Pythia, with a center-of-mass energy $\sqrt{s} = 7$ TeV and a luminosity of 20/fb. The upper (lower) plots of Fig.2 correspond to events where the Higgs decayed into $\tau\bar{\tau}$ (a pair of b-jets, $j_b j_b$). The left (right) plots are obtained in the CM χ (LAB) frame. We emphasize that this example is just for illustrative purposes. For this reason we have not incorporated a realistic τ -reconstruction, as well as b-jet identification.

As expected, the CM χ histograms show a very clear and sharp peak (pole) around 200–220 GeV, followed by an edge. In the case of the $j_b j_b$ histogram there appear events beyond the edge due to the limited efficiency in the jet reconstruction. The corresponding LAB histograms show two (non-dramatic) differences. First, a logical spreading around the maximum; and second, a slight shift of the peak towards smaller values of E_T^v . This shift is almost invisible for the $j_b j_b$ histogram. All these effects can be explained, estimated in a semi-analytical way and kept under control, as we discuss below.

We recall that the transverse variables we are using are only affected by transverse boosts when passing from CM χ to LAB. Longitudinal boosts are irrelevant for this analysis. There are two sources of transverse boosts. First, the partonic collision will not occur in general in its center-of-mass, i.e. it will have a non-vanishing net transverse momentum, typically due to initial state radiation. Second (and more importantly) even at the center-of-mass of the partonic collision, χ_2^0 can be produced with non-vanishing transverse momentum (and opposite to that of χ_1^\pm). Next we estimate the change in the E_T^v of the events at the pole due to the non-vanishing transverse momentum of χ_2^0 in the LAB.

We will distinguish two perpendicular directions in the transverse plane: the direction along $p_T^{\chi_2^0}$ (\parallel), and the perpendicular to it (\perp). Due to the boost in the \parallel direction (we will ignore the boost in the longitudinal direction, which is irrelevant here), the visible energy changes (from CM χ to LAB) as

$$\hat{E}^v \rightarrow E^v = \gamma \hat{E}^v - \beta \gamma (\hat{p}_T^v)_\parallel \quad (3.5)$$

where $(\hat{p}_T^v)_\parallel$ is the component of the visible 3-momentum in the \parallel direction. As usual, γ and β are the parameters of the Lorentz transformation, satisfying

$$\beta \gamma = \frac{|p_T^{\chi_2^0}|}{M_{\chi_2^0}}. \quad (3.6)$$

Now, for the events *at the pole* $\hat{E}_T^v = \hat{E}_v$ in the CM χ frame [18]. This holds after the transverse boost. Hence, when going to LAB, for those events the transverse energy of those events changes as in eq.(3.5):

$$\hat{E}_T^v \rightarrow E_T^v = \gamma \hat{E}_T^v - \beta \gamma (\hat{p}_T^v)_\parallel \quad (3.7)$$

which represents a shift

$$\Delta \hat{E}_T^v = (\gamma - 1) \hat{E}_T^v - \beta \gamma (\hat{p}_T^v)_\parallel. \quad (3.8)$$

Let us estimate the size of this shift. Since for a non-relativistic boost, $\gamma - 1 \simeq \frac{1}{2} \beta^2 \gamma^2$, the second term in the r.h.s. of (3.8) will normally be the dominant one, because it scales

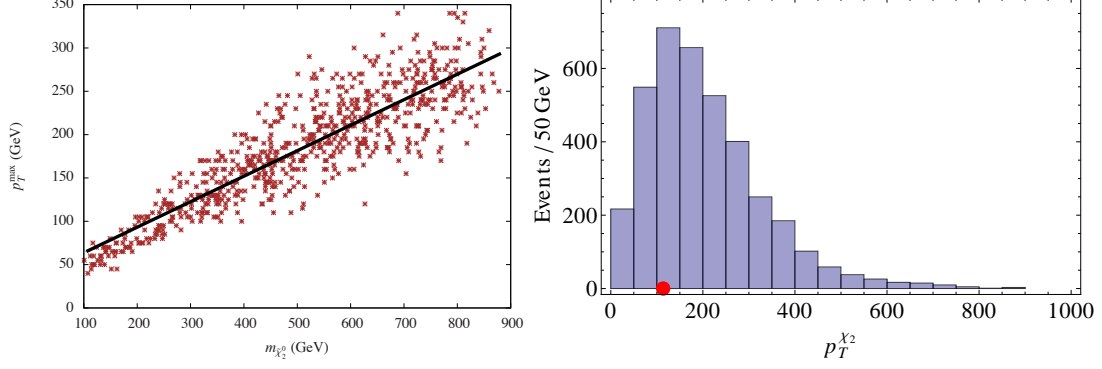


Figure 3: Left: Scatter plot of different SUSY models showing the correlation between the χ_2^0 's transverse momentum at the peak of the distribution (p_T^{\max}) and the χ_2^0 mass. The solid line shows the fitting function $p_T^{\max} = aM_{\chi_2} + b$, with $(a, b) = (0.29, 35)$. Right: p_T distribution of the χ_2 particle for a particular SUSY model with $M_{\chi_2} = 340$ GeV. The red dot shows the $p_T = M_{\chi_2}/3$ value.

with β instead of β^2 . However this term is sometimes positive and sometimes negative (depending on the sign of β), whereas the first term, which scales with β^2 , is always positive. On the other hand, in average, $(\hat{p}_T^v)_\parallel \sim \frac{1}{\sqrt{2}}\hat{p}_T^v$. Using eq.(3.4) we can express \hat{p}_T^v as a combination of the masses involved in the system,

$$(\hat{p}_T^v)^2|_{\text{pole}} = \frac{1}{4M_{\chi_2}^2} [M_{\chi_2}^2 - M_\chi^2 + M_v^2]^2 - M_v^2. \quad (3.9)$$

This gets simplified when $M_v^2 \ll M_{\chi_2}^2$, e.g. when the decay occurs via Higgs or Z -boson and also in the other cases if we select events with relatively small M_v . Therefore, at the pole

$$(\hat{p}_T^v)_\parallel \simeq \frac{1}{\sqrt{2}} \frac{1}{2M_{\chi_2}} (M_{\chi_2}^2 - M_\chi^2) \simeq \frac{1}{\sqrt{2}} \hat{E}_T^v|_{\text{pole}}, \quad (3.10)$$

which substituted back in eq.(3.8) gives

$$\Delta \hat{E}_T^v \simeq \left(\frac{1}{2}\beta^2\gamma^2 - \frac{1}{\sqrt{2}}\beta\gamma \right) \hat{E}_T^v. \quad (3.11)$$

We recall that this expression is valid for events lying at the pole, which of course are especially interesting as they provide the maximum in the histogram of the signal. Now for a numerical evaluation of $\Delta \hat{E}_T^v$ we need to estimate $\beta\gamma$. In Fig. 3 we show a scatter plot of different SUSY models, showing the correlation between the transverse momentum of χ_2^0 and its mass. As it can be checked from the fitting function, it is a good approximation to take, in average:

$$|p_T^{\chi_2}| \simeq \frac{1}{3}M_{\chi_2}. \quad (3.12)$$

This is illustrated in the right plot of Fig. 3 for a typical example. Actually this is consistent with expectations. First, the production of $\chi_1^\pm \chi_2^0$ through a W in S -channel (see Fig.1a) is dominated by the resonance. Even though the W will be normally off-shell, the penalisation for large momenta of $\chi_1^\pm \chi_2^0$ is important, although this reason becomes weaker for $M_W \ll$

$M_{\chi_2} + M_{\chi_1^\pm}$. Second, and more importantly, the PDFs penalize large energies. Since the final state particles are colourless (in this case charginos and neutralinos) with a net electric charge, they are essentially produced via quarks/antiquarks (and not gluons). This is significantly affected by the PDFs of the anti-quarks, which tend to prefer lower momenta rather than higher ones. As a consequence of these two effects, the energies of the particles at the final state are expected to be very close to their mass. This is consistent with the relation (3.12), which implies that the energy of the particle produced differs less than 5% from its mass. In consequence, from eq.(3.6, 3.12) typically $\beta\gamma \simeq 1/3$. Then eq. (3.11) becomes

$$\Delta\hat{E}_T^v = \left(\frac{1}{18} \pm \frac{1}{3\sqrt{2}} \right) \hat{E}_T^v, \quad (3.13)$$

where we have already incorporated the fact that β has a random sign. This implies a shift in the range $[-0.2\hat{E}_T^v, 0.3\hat{E}_T^v]$ in the visible transverse energy of the pole events when going from CM χ to LAB. Finally, we have to evaluate how this modifies the position of the peak. Notice that the pole events shifted positively (to the right of the histogram), will not produce any new global maximum as they fall in a region of E_T^v where there were almost no events. On the other hand the pole events shifted negatively (to the left of the histogram) will populate a region where there were already events. In addition, that region gets also populated by positive shifts of non-pole events, with lower \hat{E}_T^v values. Consequently, we expect a maximum in a value of E_T^v which is approximately 18% smaller than the value of the pole in CM χ , see eq.(3.4).

Fig.4 shows scatter plots from a large set of SUSY models, showing the correlation between the theoretical $\hat{E}_T^v|_{\text{pole}}$, given by eq.(3.4), and the actual peak value of the E_T^v -histogram, reconstructed for each SUSY model. The upper (lower) plots correspond to histograms of events where the χ_2^0 neutralinos decayed into a $\tau\bar{\tau}$ - ($j_b j_b$ -) pairs. We remark again that these plots are shown for illustrative purposes only, so no attempt of realistic identification of the τ and b -jets states is done at this level². The left (right) plots correspond to histograms in the CM χ (LAB) system. The CM χ plots show the perfect correlation of the histogram maximum and the theoretical pole (3.4). The LAB plots show the two effects expected: a certain spreading and a net shift of the average maximum with respect to the CM χ prediction. We have fitted the points of the LAB plots with simple linear functions $E_T^{\text{max}} = aE_T^{\text{pole}} + b$, getting $(a, b) = (0.79 \pm 0.02, 17 \pm 6)$, $(0.86 \pm 0.04, 22 \pm 11)$ for the $\tau\bar{\tau}$ and $j_b j_b$ cases, respectively. Note that the results for $\tau\bar{\tau}$ events are consistent with the previously discussed $\Delta\hat{E}_T^v \simeq -18\%\hat{E}_T^v$ expectation. It is remarkable, however, that for $j_b j_b$ events, the LAB results are more symmetrically distributed around the CM χ prediction. This can be easily understood by recalling that for $j_b j_b$ events the CM χ histogram does not have an end-point at the pole because of the limited efficiency in the jet reconstruction, see plot c) of Fig.2. In consequence the discussion after eq.(3.11) gets now modified since the pole $j_b j_b$ -events shifted positively fall in a region of E_T^v where there were already events. In consequence, the limited efficiency in the jet reconstruction funnily makes the position of the maximum more stable than for the leptonic histogram; thus the symmetric spreading of the LAB scatter-plot around the CM χ prediction.

²In this sense, a more realistic analysis is performed in the next subsection

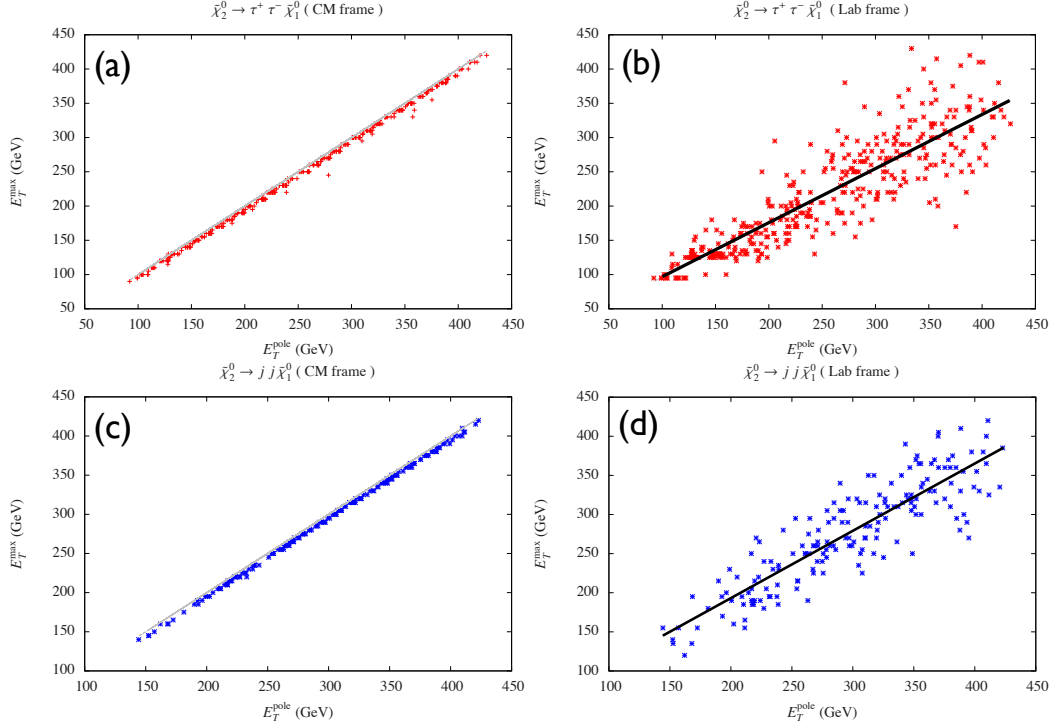


Figure 4: Scatter plot of different SUSY models showing the correlation between $E_T^v|_{\text{pole}}$ and the peak value of the variable E_T^v , reconstructed event by event for each point. This is done for the cases: a) $\tau\bar{\tau}$ pair in the CM frame; b) $\tau\bar{\tau}$ pair in the LAB frame; c) $j\bar{j}$ pair in the CM frame, and d) $j\bar{j}$ pair in the LAB frame. The straight lines show the corresponding fitting functions (see text for details).

One of the most interesting features of the E_T^v variable is that it concentrates the signal events around a maximum (determined by the supersymmetric spectrum), which does not happen for the background events (these get concentrated around M_Z , see below). This behaviour is very helpful to separate the signal events from the background events, thus improving the signal/background (S/B) ratio in the search of new physics at LHC (even before using this variable to extract information about the SUSY spectrum). It should be noticed here that the background events (typically SM production of WZ) behave as if the "neutralino" χ_2^0 had exactly the mass of the Z -boson and the "neutralino" χ_1^0 had zero-mass. Thus for the background events the peak in the E_T^v variable lies at $\sim M_Z$.

For some SUSY models, however, the position of the maximum of the signal-determined by eq.(3.4)- can be close to M_Z , i.e. the peak of E_T^v for background events. Then, the strategy to detect the existence of new-physics events can be further improved by plotting the p_T^v variable rather than E_T^v (of course, both variables are equivalent since they are unambiguously related through $E_T^v = \sqrt{M_v^2 + (p_T^v)^2}$, where M_v is a measurable quantity). Note that for the background events, the peak in p_T^v is not far from the lower kinematical cut used, while for the signal events is given by eq.(3.9), and lies normally at some non-trivial value (even if the corresponding E_T^v is close to M_Z). In the next section we will see some explicit examples where the use of the p_T^v variable is very convenient to show the

existence of new physics in the first place. Once the new physics is detected, the value of p_T^v at the maximum of the signal can be related to the SUSY spectrum through eq.(3.9) or equivalently through eq.(3.4).

Next we explore these features in further detail.

4. Testing the efficiency of E_T^v and p_T^v in concrete SUSY models

As we have described before, the chargino-neutralino pair production can be studied through the use of the visible transverse energy, E_T^v , regardless of the way the neutralino χ_2^0 has decayed. So here we only care about initial and final states.

We will simulate LHC signals with $\sqrt{s} = 14$ TeV and luminosity of 100/fb, using the package **SUSY-HIT** [19, 20, 21, 22], as well as **SOFTSUSY**[23] for the spectrum calculators, and **MadGraph** /**MadEvent** [24] and **PYTHIA**[25] for the event simulation. We focus on events with 3 leptons + missing transverse momentum, and apply the following general cuts

- the existence of at least two identical, opposite signed leptons
- the 3rd hardest lepton having $E_T > 10$ GeV
- At least an electron (muon) with $E_T > 25$ GeV ($p_T > 20$ GeV)
- 3 leptons with $p_T > 20$ GeV and $\eta < 2.47$ for electrons ($\eta < 2.4$ for muons)
- $E_T^{\text{miss}} > 50$ GeV
- The transverse mass of the 2nd chain $M_T > 90$ GeV, ³
- Jets $p_T < 20$ GeV
- PGS ATLAS cuts [24] .

The jet reconstruction is performed using the anti- k_T algorithm with $\Delta R = 0.4$, whereas the Initial State Radiation is simulated directly from the Matrix Element, with Parton Shower matching implemented by **Madgraph**/**MadEvent** by making use of MLM methods. We illustrate our strategy by working in the context of the MSSM. Specifically we choose the following SUSY models (defined at the M_Z scale)

$$\begin{aligned}
\text{Model 1 :} & \quad M_1 \simeq 99 \text{ GeV}, \quad M_2 \simeq 183 \text{ GeV}, \quad \mu \simeq 705 \text{ GeV}, \quad \tan \beta = 10, \\
\text{Model 2 :} & \quad M_1 \simeq 47 \text{ GeV}, \quad M_2 \simeq 244 \text{ GeV}, \quad \mu \simeq -515 \text{ GeV}, \quad \tan \beta = 19, \\
\text{Model 3 :} & \quad M_1 \simeq 93 \text{ GeV}, \quad M_2 \simeq 405 \text{ GeV}, \quad \mu = -5372 \text{ GeV}, \quad \tan \beta = 50
\end{aligned} \tag{4.1}$$

where M_1, M_2 are the bino and wino mass parameters at low-energy, and $\tan \beta \equiv \langle H_u \rangle / \langle H_d \rangle$ is the ratio between the VEVs of the two Higgs doublets. We do not specify the values of gluino and sfermion masses, which are assumed to be heavy (note that we are not imposing

³Computed with the unpaired lepton, see discussion below.

gaugino-mass unification). In the three models we study the signal of χ_2^0 decaying through a Z -boson, which is the dominant one for all of them (more details below). The dominant background is WZ and WZ +jet production in the SM.

The strategy of the analysis for the three models is the following:

- We reconstruct the possible invariant masses M_v of a pair of identical leptons, selecting the events where a pair of opposite-sign leptons has an invariant mass close to M_Z

$$M_v = M_Z \pm 10 \text{ GeV} .$$

This pair is identified as a daughter of a Z , thus the third lepton, ℓ' , should come from a W . This holds for both the signal and the SM background.

It is important to note that most of the WZ background events are actually removed thanks to the $M_T > 90 \text{ GeV}$ requirement in the above list of cuts. The reason is the following. Taking into account that for the events of the background the missing momentum can be identified with the neutrino, one constructs the associated transverse mass, which satisfies the following inequality

$$(M_T^{\ell'\nu})^2 = (E_T^{\ell'} + E_T^\nu)^2 - (\vec{p}_T^{\ell'} + \vec{p}_T^\nu)^2 \leq M_W^2 , \quad (4.2)$$

where ℓ' is the charged lepton coming from the W (i.e. the unpaired lepton). Hence, identifying p_T^{miss} with p_T^ν and discarding events with $M_T^{\ell'\nu} < M_W$ would in principle remove the whole WZ background. Although, due to the inefficiency in the reconstruction of the missing piece, some background events may violate in practice the inequality (4.2). This turns out to be an extremely efficient constraint to improve the S/B ratio.

- With the surviving events, we reconstruct the E_T^v , p_T^v variables associated to the lepton pair daughter of the Z .
- We simulate the background taking into account only the contribution from WZ and WZ +jet production, which is by far the dominant one in the regions of interest (see e.g. [10]). We have checked that the results of our simulations are in agreement with [10].
- Finally, we construct the E_T^v , p_T^v histograms to show the signal over the background.

Next we expound the results obtained for the three models considered, in a separate way.

Model 1

From the initial parameters listed in eq.(4.1), we obtain the relevant supersymmetric spectrum for the analysis, which reads

$$M_{\chi_1^\pm} \simeq 207 \text{ GeV}, \quad M_{\chi_2^0} \simeq 203 \text{ GeV}, \quad M_{\chi_1^0} \simeq 107 \text{ GeV}. \quad (4.3)$$

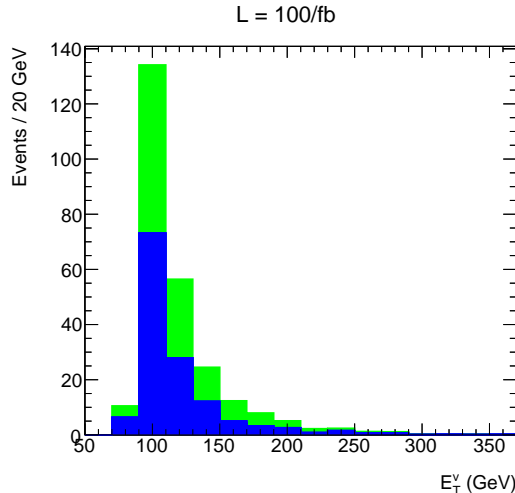


Figure 5: Histogram (in number of events) of E_T^v for the parameters corresponding to Model 1 (see text), taking into account the signal plus the dominant background (W/Z production).

Since the staus are heavy, a priori the preferred decay channel of χ_2^0 is through the lightest Higgs, $m_h = 126$ GeV. However, since $M_{\chi_2} - M_\chi < m_h$, this channel is suppressed and the favourite decay-channel turns out to be through an on-shell Z . As mentioned above, the main background for this final-state topology is the SM production of a W/Z pair.

Fig.5 shows the histogram corresponding to the variable E_T^v , considering the background plus the signal with a luminosity of 100/fb, which will be reached in the near future. The SUSY signal is clearly visible. The position of its peak can be used to extract information about the SUSY spectrum in the way discussed in sect. 3. More precisely, for this model the prediction of eq.(3.4) for the visible transverse energy at the pole of the signal is $\hat{E}_T^v|_{\text{pole}} \simeq 94$ GeV, which is consistent with the bin of the histogram corresponding to the maximum signal, i.e. 90 GeV – 110 GeV.

This case illustrates the possibility that the peak of the E_T^v –histogram for the signal lies close to the peak for the background, i.e. M_Z . Note from Fig. 5 that both peaks are at the same bin, as expected.

As discussed at the end of sect. 3, this feature can be improved by plotting p_T^v instead of E_T^v . The result is shown in Fig.4 (top-left plot). Note that the peak of the signal (the bin centered at 50 GeV) is now displaced with respect to the background one (the bin at 30 GeV), which represents a certain (though admittedly non-dramatic) improving. Fig.4 (top-right plot) shows the p_T^v –histogram of just the signal events. Of course, it is not something one can realistically obtain from the experiment but we present it in order to show the shape of the signal events, gathered around the (theoretically predicted) maximum.

For the sake of comparison we have presented in Fig. 4 (bottom) the analogous plots for the missing momentum variable, p_T^{miss} , which is used in the experimental searches of ATLAS and CMS. The p_T^v variable turns out to be slightly better in the S/B ratio, showing that it can be at least as efficient as p_T^{miss} for the initial task of detecting the presence of new

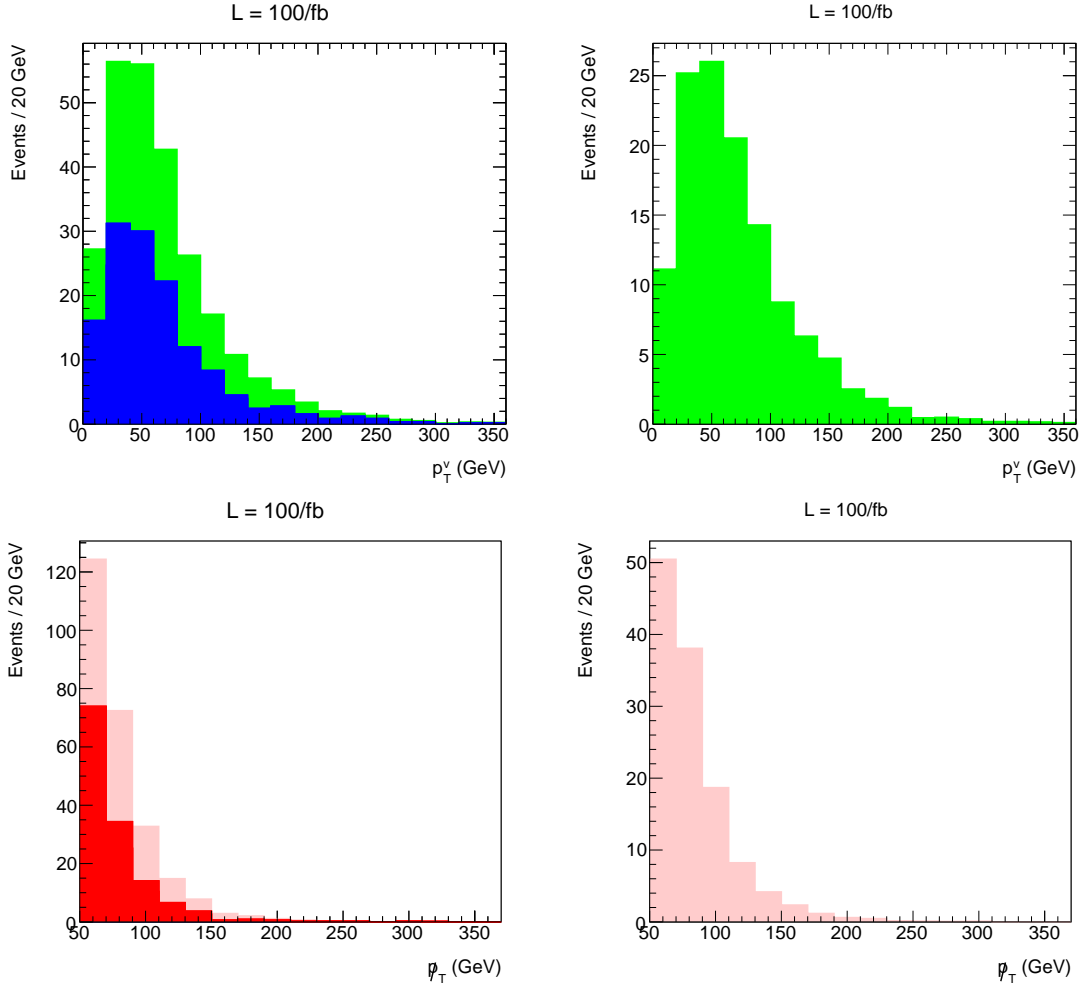


Figure 6: Top- (bottom-) left: the same as in Fig. 5 but now for the p_T^v

physics. Besides, in contrast with p_T^{miss} , the measure of p_T^v is direct and presumably less affected by systematic uncertainties. And, furthermore, once the presence of new physics is recognized, the p_T^v variable provides valuable information about its spectrum since the maximum of the signal in is related to a defined combination of the supersymmetric masses, eq. (3.9).

Model 2

In this case the relevant supersymmetric spectrum reads

$$M_{\chi_1^\pm} \simeq 273 \text{ GeV}, \quad M_{\chi_2^0} \simeq 273 \text{ GeV}, \quad M_{\chi_1^0} \simeq 53 \text{ GeV}. \quad (4.4)$$

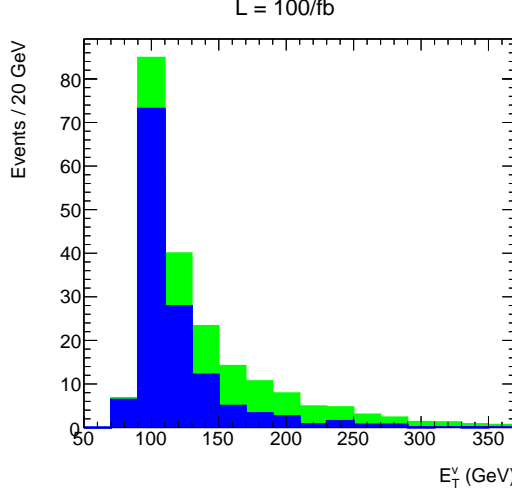


Figure 7: The same as Fig. 5, but here for Model 2 (see text).

χ_2^0 and χ_1^0 are almost pure bino and wino respectively. Now the decay of χ_2^0 through an on-shell Higgs is kinematically allowed, so one would expect it to be the preferred decay channel. However, the branching ratio of the decays through a Higgs or through a Z -boson are 39% and 61% respectively. The reason is the following. Due to the relatively high value of $\tan \beta$, the χ_2^0 and χ_1^0 neutralinos are essentially gauginos with a small \tilde{H}_d^0 component and a *very* small \tilde{H}_u^0 component. On the other hand, the physical Higgs-boson is essentially H_u^0 for the same reason. Then the χ_2^0 decay through a Higgs occurs thanks to those very small \tilde{H}_u^0 components and gets suppressed, while the decay through a Z -boson may occur also through the not-so-small \tilde{H}_d^0 components of the neutralinos.

Fig. 7 shows the histogram corresponding to the variable E_T^v , containing the background plus the signal, again with a luminosity of 100/fb. The SUSY signal is of course weaker than in Model 1, since the supersymmetric masses are larger. On the other hand, it is nice that now the peak of the signal does not coincide with the peak of the background. In this case eq.(3.4) gives $\hat{E}_T^v|_{\text{pole}} \simeq 146 \text{ GeV}$, consistent with what the signal peak visible at Fig. 7.

As for Model 1, in this case the separation between the signal and background peaks is more efficiently achieved using the variable p_T^v rather than E_T^v , as it is shown in Fig.8 (top plots). We show also the analogous plots for p_T^{miss} . Again the behavior is slightly better for p_T^v , in particular in the region of higher statistics.

Model 3

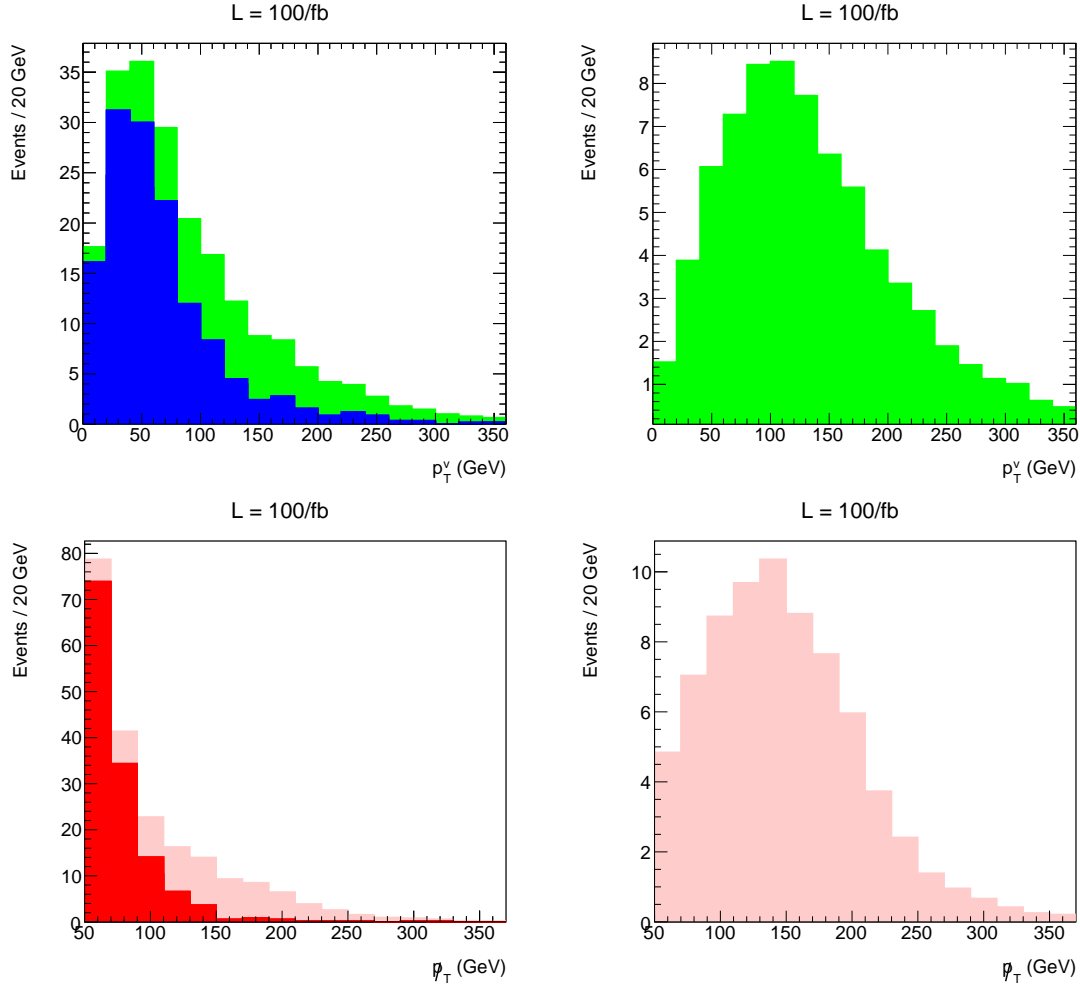


Figure 8: The same as Fig. 6, but here for Model 2 (see text).

Finally, for Model 3 the spectrum reads

$$M_{\chi_1^\pm} \simeq 405.3 \text{ GeV}, \quad M_{\chi_2^0} \simeq 405.3 \text{ GeV}, \quad M_{\chi_1^0} \simeq 94 \text{ GeV}. \quad (4.5)$$

Again here χ_2^0 and χ_1^0 are almost purely wino and bino respectively, with very small Higgsino components of $\mathcal{O}(\lesssim 10^{-2})$. Also in this case the neutralinos contain much more \tilde{H}_d^0 than \tilde{H}_u^0 , leading to branching ratios $\text{BR}(\chi_2^0 \rightarrow \chi_1^0 h)$ and $\text{BR}(\chi_2^0 \rightarrow \chi_1^0 Z)$ to be 4% and 96% respectively, for similar reasons as before. Since now $\tan \beta$ is much larger the Higgs channel is even more suppressed.

Fig. 9 and Fig. 10 show the histograms in the E_T^v and the p_T^v, p_T^{miss} variables respectively. They show similar features as for Model 2. The difference of course is that the signal is now quite small due the large supersymmetric masses. Still it is visible, especially for the p_T^v variable. Since the S/B ratio is high (~ 2) around the p_T^v -peak of the signal, the later would be visible with larger luminosities (say 300/fb).

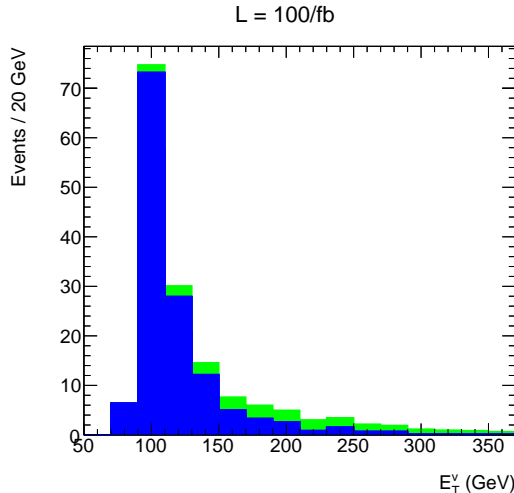


Figure 9: The same as Figs. 5, 7, but here for Model 3 (see text).

5. Conclusions

The study of chargino-neutralino pair production at the LHC finds nowadays an unprecedented motivation, since the detection of those particles could well represent an opportunity of discovering light supersymmetric states at the LHC. Different strategies have been used so far by the experimental groups ATLAS and CMS to explore this process. They have been mainly focused on the analysis of 3-leptons plus missing-energy final states using standard kinematical variables, such as p_T^{miss} and the invariant mass $m_{\ell^+\ell^-}$.

In this work, we have presented a new -purely kinematical- method based on the variable $E_T^v = \sqrt{M_v^2 + (p_T^v)^2}$, i.e. the transverse energy of the visible products coming from the neutralino (typically two leptons or two b-jets), which presents some very useful features. First of all, the histogram in E_T^v (in the frame where the decaying neutralino is at rest) has a pole. This translates into a peak in the actual experimental distribution. Consequently, this is a very robust feature against poor statistics. In addition, this concentration of signal-events around the maximum does not occur for the background-events. In this sense, it is highly advantageous to use, instead of E_T^v , the equivalent variable p_T^v (transverse momentum of the visible decaying products). This optimizes the S/B ratio, showing a (slightly) better performance than the usual p_T^{miss} variable. Furthermore, the main merit of the E_T^v or p_T^v variables is that the peak in the histogram is correlated in a well-defined way to a precise combination of SUSY masses, given by

$$E_T^v|_{\text{pole}} = \frac{1}{2M_{\chi_2}} [M_{\chi_2}^2 - M_{\chi_1}^2 + M_v^2] , \quad (5.1)$$

$$(p_T^v)^2|_{\text{pole}} = (E_T^v)^2|_{\text{pole}} - M_v^2 . \quad (5.2)$$

where M_{χ_2} , M_{χ_1} and M_v are the masses of the decaying neutralino χ_2^0 , the lightest neutralino (LSP) and the visible system to which χ_2^0 decays to.

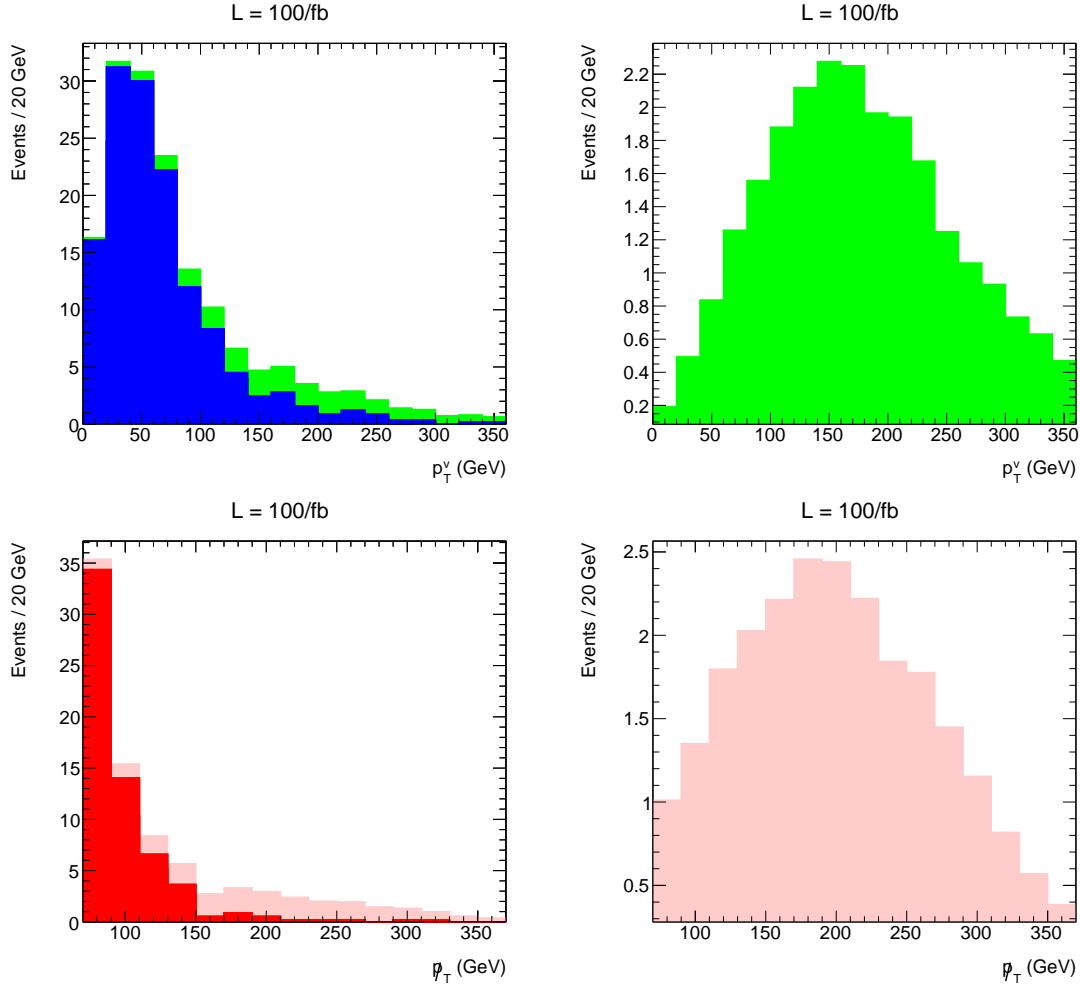


Figure 10: The same as Fig. 6, 8, but here for Model 3 (see text).

Of course, when passing from the CM_χ to the LAB system the maximum becomes less sharp and the position of the maximum is slightly shifted. However, these effects are not dramatic and, besides, can be well estimated in a semi-analytical way and kept under control.

We have illustrated these facts performing a realistic analysis of particular SUSY models, where the χ_2^0 neutralino decays mainly through a Z boson. We have focussed in events where the final state consists of 3 leptons plus missing energy, showing that the SUSY signal in the p_T^ν variable could be very well detected at the LHC running with 14 TeV and a luminosity of 100/fb, which is attainable in the near future.

Let us finally stress that the same method can be applied to any possible decay channel of χ_2^0 : through squark, sleptons or a Higgs. The latter case is actually the most frequent one for MSSM models. Then, the most probable final state contains 2 b-jets, 1 lepton (or jet) and missing energy. The $h \rightarrow b\bar{b}$ channel has the additional advantage of having large branching ratios compared to the $Z \rightarrow \ell\bar{\ell}$ case. On the other hand, the topology $j_b j_b \ell$ is

much less clean and difficult to reconstruct properly. Thus it requires a separate study which is out of the scope of the present paper and will be the subject of a future research work.

Acknowledgements

We are grateful to Krzysztof Rolbiecki and Paul de Jong for very useful discussions. This work has been partially supported by the MICINN, Spain, under contract FPA2010-17747; Consolider-Ingenio PAU CSD2007-00060, CPAN CSD2007-00042. We thank as well the Comunidad de Madrid through Proyecto HEPHACOS S2009/ESP-1473 and the European Commission under contract PITN-GA-2009-237920. M. E. Cabrera acknowledges the financial support of the CSIC through a predoctoral research grant (JAEPRe 07 00020); and the ERC “WIMPs Kairos - the moment of truth for wimp dark matter” (P.I. Gianfranco Bertone). The work of A. Casas has been partially supported by the MICINN, Spain, under contract FPA2010-17747 and the Consolider-Ingenio PAU CSD2007-00060, CPAN CSD2007-00042. We thank as well the Comunidad de Madrid through Proyecto HEPHACOS S2009/ESP-1473 and the European Commission under contract PITN-GA-2009-237920.

References

- [1] F. Gianotti, *Update on the Standard Model Higgs searches in ATLAS*, [ATLAS-CONF-2012-093](#).
- [2] J. Incandela, *Update on the Standard Model Higgs searches in CMS*, [CMS-PAS-HIG-12-020](#).
- [3] M. Farina, M. Kadastik, D. Pappadopulo, J. Pata, M. Raidal, et al., *Implications of XENON100 and LHC results for Dark Matter models*, *Nucl.Phys.* **B853** (2011) 607–624, [[arXiv:1104.3572](#)].
- [4] C. Balazs, A. Buckley, D. Carter, B. Farmer, and M. White, *Should we still believe in constrained supersymmetry?*, [arXiv:1205.1568](#).
- [5] S. Akula, P. Nath, and G. Peim, *Implications of the Higgs Boson Discovery for mSUGRA*, *Phys.Lett.* **B717** (2012) 188–192, [[arXiv:1207.1839](#)].
- [6] O. Buchmueller, R. Cavanaugh, M. Citron, A. De Roeck, M. Dolan, et al., *The CMSSM and NUHM1 in Light of 7 TeV LHC, Bs to mu+mu- and XENON100 Data*, *Eur.Phys.J.* **C72** (2012) 2243, [[arXiv:1207.7315](#)].
- [7] A. Arbey, M. Battaglia, A. Djouadi, and F. Mahmoudi, *The Higgs sector of the phenomenological MSSM in the light of the Higgs boson discovery*, *JHEP* **1209** (2012) 107, [[arXiv:1207.1348](#)].
- [8] C. Stenge, G. Bertone, F. Feroz, M. Fornasa, R. Ruiz de Austri, et al., *Global Fits of the cMSSM and NUHM including the LHC Higgs discovery and new XENON100 constraints*, *JCAP* **1304** (2013) 013, [[arXiv:1212.2636](#)].
- [9] M. E. Cabrera, J. A. Casas, and R. R. de Austri, *The health of SUSY after the Higgs discovery and the XENON100 data*, [arXiv:1212.4821](#).

- [10] **ATLAS Collaboration** Collaboration, G. Aad et al., *Search for supersymmetry in events with three leptons and missing transverse momentum in $\sqrt{s} = 7$ TeV pp collisions with the ATLAS detector*, *Phys.Rev.Lett.* **108** (2012) 261804, [[arXiv:1204.5638](#)].
- [11] **CMS Collaboration** Collaboration, S. Chatrchyan et al., *Search for electroweak production of charginos and neutralinos using leptonic final states in pp collisions at $\sqrt{s} = 7$ TeV*, *JHEP* (2012) [[arXiv:1209.6620](#)].
- [12] **ATLAS Collaboration** Collaboration, G. Aad et al., *Expected Performance of the ATLAS Experiment - Detector, Trigger and Physics*, [arXiv:0901.0512](#).
- [13] A. J. Barr and C. G. Lester, *A Review of the Mass Measurement Techniques proposed for the Large Hadron Collider*, *J.Phys.* **G37** (2010) 123001, [[arXiv:1004.2732](#)].
- [14] M. M. Nojiri and Y. Yamada, *Neutralino decays at the CERN LHC*, *Phys.Rev.* **D60** (1999) 015006, [[hep-ph/9902201](#)].
- [15] U. De Sanctis, T. Lari, S. Montesano, and C. Troncon, *Perspectives for the detection and measurement of supersymmetry in the focus point region of mSUGRA models with the ATLAS detector at LHC*, *Eur.Phys.J.* **C52** (2007) 743–758, [[arXiv:0704.2515](#)].
- [16] B. Gjelsten, . Miller, D.J., and P. Osland, *Measurement of SUSY masses via cascade decays for SPS 1a*, *JHEP* **0412** (2004) 003, [[hep-ph/0410303](#)].
- [17] A. Birkedal, R. Group, and K. Matchev, *Slepton mass measurements at the LHC*, *eConf* **C050318** (2005) 0210, [[hep-ph/0507002](#)].
- [18] M. E. Cabrera and J. A. Casas, *Understanding and improving the Effective Mass for LHC searches*, [arXiv:1207.0435](#).
- [19] A. Djouadi, J.-L. Kneur, and G. Moultaka, *SuSpect: A Fortran code for the supersymmetric and Higgs particle spectrum in the MSSM*, *Comput.Phys.Commun.* **176** (2007) 426–455, [[hep-ph/0211331](#)].
- [20] M. Muhlleitner, A. Djouadi, and Y. Mambrini, *SDECAY: A Fortran code for the decays of the supersymmetric particles in the MSSM*, *Comput.Phys.Commun.* **168** (2005) 46–70, [[hep-ph/0311167](#)].
- [21] A. Djouadi, J. Kalinowski, and M. Spira, *HDECAY: A Program for Higgs boson decays in the standard model and its supersymmetric extension*, *Comput.Phys.Commun.* **108** (1998) 56–74, [[hep-ph/9704448](#)].
- [22] A. Djouadi, M. Muhlleitner, and M. Spira, *Decays of supersymmetric particles: The Program SUSY-HIT (SuSpect-Sdecay-Hdecay-InTerface)*, *Acta Phys.Polon.* **B38** (2007) 635–644, [[hep-ph/0609292](#)].
- [23] B. Allanach, *SOFTSUSY: a program for calculating supersymmetric spectra*, *Comput.Phys.Commun.* **143** (2002) 305–331, [[hep-ph/0104145](#)].
- [24] J. Alwall, M. Herquet, F. Maltoni, O. Mattelaer, and T. Stelzer, *MadGraph 5 : Going Beyond*, *JHEP* **1106** (2011) 128, [[arXiv:1106.0522](#)].
- [25] T. Sjostrand, S. Mrenna, and P. Z. Skands, *PYTHIA 6.4 Physics and Manual*, *JHEP* **0605** (2006) 026, [[hep-ph/0603175](#)].